Rheol Acta (2005) 45: 151–163
DOI 10.1007/s00397-005-0033-7

ORIGINAL CONTRIBUTION

Jens Hepperle
Helmut Münstedt
Peter K. Haug
Claus D. Eisenbach

Rheological properties of branched polystyrenes: linear viscoelastic behavior

Received: 16 March 2004
Accepted: 21 March 2005
Published online: 5 November 2005

This article has already been published online first (DOI: http://dx.doi.rog/10.1007/s00397-005-0005-y). Due to an oversight at the publisher's, this version contained several mistakes. The article is herewith republished in its entirety as a "publisher's erratum".

Electronic Supplementary Material Supplementary material is available for this article at http://dx.doi.org/10.1007/s00397-005-0033-7

J. Hepperle · H. Münstedt (✉)
Institute of Polymer Materials, University Erlangen-Nürnberg, Martensstr. 7, 91058 Erlangen, Germany
E-mail: helmut.muenstedt@ww.uni-erlangen.de

P. K. Haug · C. D. Eisenbach
Institute of Applied Macromolecular Chemistry, University of Stuttgart, Pfaffenwaldring 55, 70569 Stuttgart, Germany

Present address: J. Hepperle
Bayer Technology Services GmbH, 51368 Leverkusen, Germany
E-mail: jens.hepperle@bayertechnology.com

Abstract Oscillatory shear measurements on a series of branched graft polystyrenes (PS) synthesized by the macromonomer technique are presented. The graft PS have similar molar masses (M_w between 1.3×10^5 g/mol and 2.4×10^5 g/mol) and a polydispersity M_w/M_n around 2. The molar masses of the grafted side chains $M_{w,\mathrm{br}}$ range from 6.8×10^3 g/mol to 5.8×10^4 g/mol, which are well below and above the critical entanglement molar mass M_c of linear polystyrene. The average number $\bar{p}$ of side chains per molecule ranges from 0.6 to 6.7. The oscillatory measurements follow the time–temperature superposition principle. The shift factors do not depend on the number of branches. The zero-shear viscosities of all graft PS are lower than those of linear PS with the same molar mass, which can be attributed to the smaller coil size of the branched molecules. It is shown that the influence of branching on the frequency dependence of the dynamic moduli is weak for all graft PS that were investigated, which can be explained by the low entanglement density.

Keywords Graft polystyrenes · Long-chain branching · Dynamic-mechanical experiments · Temperature dependence · Viscosity functions

Introduction

Molar masses, their distribution and long-chain branching have a pronounced influence on rheological properties of polymer melts. An increasing strain hardening, a higher melt elasticity and a higher degree of shear thinning are reported for long-chain branched polyethylenes and polypropylenes compared to the properties of linear polymers (Münstedt and Laun 1981; Kurzbeck et al. 1999). In the case of polyethyl-

enes, long-chain branches increase the flow-activation energy and lead to a higher temperature dependence of rheological properties (Gabriel and Münstedt 1999; Laun 1987).

In most cases, the branching of commercial polymers is random due to the polymerization techniques used. As an example, random branching is caused by chain-transfer in the radical polymerization of low-density polyethylene (LDPE) as mentioned by Odian (1991), incorporation of vinyl-terminated chains in metallocene-catalyzed polyethylene (Harrison et al. 1998; Tobita 1999; Beigzadeh et al. 1999) or by crosslinking reactions with multifunctional monomers (Ferri and Lomellini 1999). For these randomly branched polymers, the molecular topology is not known in detail. In addition, randomly branched polymers show a broader polydispersity in many cases, which makes an interpretation of the influence of branching on rheological properties to be difficult (Kurzbeck et al. 1999; Ferri and Lomellini 1999).

Therefore, the effect of long-chain branching on rheological properties was studied on narrow-distributed model polymers, such as stars (Pryke et al. 2002; Lee and Archer 2002; Islam et al. 2001; Graessley and Roovers 1979; Pearson et al. 1983), H-shaped polymers (Roovers 1984) and combs (Daniels et al. 2001; Roovers and Graessley 1981; Fujimoto et al. 1972). Most of the studies on branched model systems were carried out on stars, but combs and H-shaped polymers are investigated to get a more realistic approach towards the randomly branched topologies of commercial polymers.

The objective of this paper is to examine rheological properties of polystyrene (PS) graft polymers with similar molar masses and molar mass distributions, but with varying average numbers of grafted side chains per molecule and different molar masses. One aim is to investigate the effect of the number of branches and their molar mass on linear-viscoelastic properties of the melts. Varying molar masses of the grafted side chains above and well below the critical molar mass $M_c \cong 1M_e$ for the formation of entanglements of linear chains allow a study of the change in rheological properties from entangled to unentangled side chains. M_e is the molar mass of a polymer strand between two entanglements.

Experimental

The synthesis of the graft PS by copolymerization of methacryloyl-terminated polystyrene macromonomers and styrene is already described in detail elsewhere (Haug 2000).

After the synthesis and purification by reprecipitation, the graft PS were dissolved in benzene and 0.1 wt% of a stabilizer (Irganox 1076) was added; the solution was freeze-dried to give a fine powder. The freeze-dried powders were kept under vacuum at $T = 80°C$ for at least 48 h to remove residual solvents. The content of volatile organic compounds of the dried powders was checked using headspace analysis with a gas chromatograph. For all dried samples the content of volatile organic compounds was less than 35 ppm or not detectable. A possible influence of the stabilizer and the dissolution procedure on rheological properties was checked with a commercial polystyrene sample, which was dissolved together with the stabilizer and dried in the same way as the synthesized materials (Hepperle 2002). No significant differences in the dynamic moduli at 170°C and 200°C between the pellets as received from the manufacturer and the stabilized powder were observed.

For the characterization of the molecular mass distribution, a room-temperature size exclusion chromatograph (SEC) with four columns (Waters, pore size: 10^6, 10^5, 10^4, 10^3 Å) and a refractive index-detector were used. The temperature for the measurements was $T = 25°C$, the solvent used was THF with a flow rate of 0.5 ml/min. The columns were calibrated with 13 narrowly distributed polystyrene standards from Polymer Laboratories with molar masses ranging from 5.8×10^2 g/mol to 1.16×10^7 g/mol. Static light scattering measurements were performed as described by Haug (2000). Solution viscosities were determined with an Ubbelohde viscometer. Dilute solutions of the sample in toluene with five concentrations in a range between 1 mg/ml and 10 mg/ml were used for the determination of the intrinsic viscosity $[\eta]$.

For shear rheology, the dried powders were compression moulded in a vacuum oven at 170°C to form discs of a diameter of 20 mm and a height of about 1.8 mm. Oscillatory shear experiments to determine the thermal stability were carried out using a controlled-stress rheometer (CS-Melt, Bohlin Instruments) with a cone and plate geometry (plate diameter: $d = 25$ mm, cone angle: 2.5°). Shear stresses between $\tau = 1$ Pa and $\tau = 10$ Pa were applied, which lead to deformations within the linear-viscoelastic range. The investigations of thermal stability were performed at a temperature of $T = 220°C$ under nitrogen atmosphere and at an angular frequency of $\omega = 0.1$ rad/s.

The small-strain oscillatory shear measurements were carried out using an ARES rheometer (Rheometric Scientific) with a cone and plate geometry (plate diameter of 25 mm and cone angle of 5.73°). The cone and plate geometry was chosen to reduce the amount of material needed. Dynamic-mechanical experiments were performed at temperatures between 140°C and 220°C under nitrogen atmosphere over an angular frequency range of 0.15 rad/s $< \omega <$ 100 rad/s.

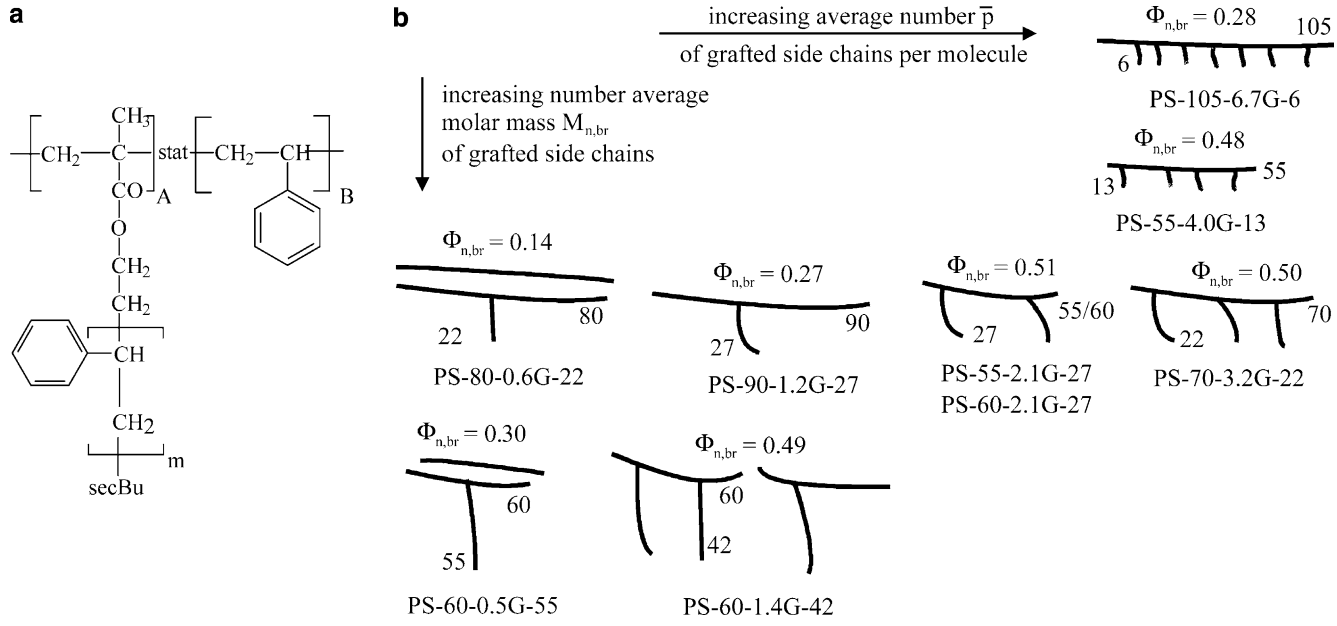

Fig. 1 **a** Chemical structure of the PS graft polymers. The grafted side chains are statistically distributed along the backbone. **b** Sketch of the constitution of PS graft polymers. The nomenclature denotes the topology of the graft polymer which is described as PS $-x-\bar{p}$G $-y$. The symbol x denotes the number average molar mass of the backbone $M_{n,\mathrm{bb}}$ (kg/mol), y denotes $M_{n,\mathrm{br}}$ of the grafted side chains (kg/mol) and $\bar{p}$ denotes the average number of grafted chains per molecule. $\Phi_{n,\mathrm{br}}$ is the number-average fraction of grafted side chains according to Eq. 1. The second figures of PS-80-0.6G-22, PS-60-0.5G-55 and PS-60-1.4G-42 indicate that all graft polymers consist of a mixture with different topologies and that the number $\bar{p}$ of grafted side chains is a mean value

Results and discussion

Materials

Polystyrene graft polymers were synthesized in a two-step polymerization (Haug 2000). The first polymerization comprises the synthesis of macromonomers by anionic polymerization of styrene and a functionalization to introduce the reactive end group. The macromonomers are then radically copolymerized with styrene. The resulting chemical structure is shown in Fig. 1a. By variation of the macromonomer molar mass and the ratio of macromonomer to styrene, different graft PS were obtained, whose topologies are illustrated in Fig. 1b. Their molecular structure can best be described as a mixture of linear chains, asymmetric stars and brushes, i.e., grafted side chains of a relatively narrow molar mass distribution are randomly attached to the backbone (for combs, an equal distance between branch points would be necessary). The molar mass and molar mass distribution of the backbones were obtained by SEC after selective ester cleavage of the side chains (Haug 2000). The backbone length distribution is not as narrow as the graft length distribution due to the free radical copolymerization of styrene with the macromonomers, which have been synthesized by living anionic polymerization. Molecular data are summarized in Table 1.

One objective of the graft polymer synthesis was to obtain graft PS with similar molar masses and polydispersities, but with varying average numbers and molar masses of the grafted side chains. The constitution of the sample is described as PS $-x-\bar{p}$G $-y$ with x describing the average number of molecular mass $M_{n,\mathrm{bb}}$ (kg/mol) of the backbone, $\bar{p}$ the average number of the grafted side chains per molecule randomly attached to the backbone and y the number average molar mass $M_{n,\mathrm{br}}$ (kg/mol) of the side chains.

Coupled SEC-viscometry shows a decreased (online) intrinsic viscosity of the graft PS in comparison with linear PS of identical molar masses (Haug 2000). The difference of the intrinsic viscosity between the linear and the branched PS increases with rising molar mass, suggesting that the amount of grafted side chains increases with molar mass.

The determination of the molar mass for strands between entanglements M_e from the plateau modulus G_N^0 of linear PS gives a value of 18,100 g/mol (Ferry 1980). To investigate the rheological properties resulting from entangled and non-entangled side chains, the side chain molar masses $M_{w,\mathrm{br}}$ were varied to be well below and above $M_c \cong 31{,}200$ g/mol, the critical molecular weight for the entanglement of linear chains (Ferry 1980). As shown in Table 1, the graft polymers can be divided into four groups, depending on the molar masses

Table 1 Molecular parameters of linear and graft PS

Sample	$\bar{p}^a$	w^b_{MM}	Grafted side chains				Backbone			Graft polymer		
			$\Phi^c_{n,br}$	$M^d_{w,br}$ (g/mol)	$M_{w,br}/M^d_{n,br}$	n^e_{br}	$M_{w,bb}{}^f$(g/mol)	$M_{w,bb}/M_{n,bb}$	n^e_{bb}	$M^g_{w,LS}$(g/mol)	$M_{w,SEC}$(g/mol)	M_w/M_n
PS-60-1.4G-42	1.4	0.17	0.49	45,400	1.07	2.5	93,000	1.63	5.1	159,600	145,100	1.66
PS-60-0.5G-55	0.5	0.07	0.30	58,300	1.05	3.2	112,000	1.82	6.2	148,400	146,900	1.73
PS-60-0.5G-55*	0.5	0.23	0.30	58,300	1.05	3.2	112,000	1.82	6.2	134,400	133,200	1.71
PS-70-3.2G-22	3.2	0.24	0.50	22,710	1.05	1.3	105,900	1.49	5.9	156,400	126,300	2.35
PS-60-2.1G-27	2.1	0.01	0.49	28,650	1.03	1.6	85,300	1.36	4.7	164,500	146,700	1.42
PS-55-2.1G-27	2.1	0.12	0.51	28,650	1.03	1.6	80,500	1.49	4.4	150,300	126,100	1.94
PS-90-1.2G-27	1.2	0.05	0.27	28,650	1.03	1.6	136,600	1.49	7.5	177,500	161,900	1.83
PS-90-1.2G-27*	1.2	0.15	0.27	28,650	1.03	1.6	136,600	1.49	7.5	150,700	129,100	2.42
PS-80-0.6G-22	0.6	0.06	0.14	22,710	1.05	1.3	122,100	1.54	6.7	131,900	130,600	1.89
PS-55-4.0G-13	4.0	0.04	0.48	14,170	1.03	0.8	82,200	1.48	4.5	155,100	135,200	1.80
PS-105-6.7G-6	6.7	0.01	0.28	6,800	1.09	0.4	158,600	1.52	8.8	236,400	192,400	1.90
PS-r-95	0	–	–	–	–	–	157,000	1.65	8.7	–	–	–

[a]Average number of branches per molecule
[b]Mass fraction of residual macromonomer, determined by SEC-peakfitting (Haug 2000)
[c]Number-average mass fraction of the side chains in the branched polymer, calculated with Eq.1
[d]Molecular data of the macromonomers before reaction, determined by SEC
[e]Average number of entanglements of grafted side chains and of the backbone determined using $n_{br} = M_{w,br}/M_e$ and $n_{bb} = M_{w,bb}/M_e$, respectively. $M_e = 18{,}100$ g/mol (Ferry 1980)
[f]Mass-average molar mass of the backbone polymer, determined by peakfitting analysis of the SEC trace after ester cleavage of the grafted side chains (Haug 2000)
[g]Mass-average molar mass determined by static light scattering (Haug 2000)

of the grafted side chains and the number of entanglements n_{br}: two graft PS with a mass-average molar mass of the side chains $M_{w,br}$ which is well above $2M_e$ (PS-60-1.4G-42, PS-60-0.5G-55), four with side chains of $2M_e > M_{w,br} > M_e$ (PS-70-3.2G-22, PS-60-2.1G-27/PS-55-2.1G-27, PS-90-1.2G-27 and PS-80-0.6G-22), one with side chains close to or slightly below M_e (PS-55-4.2G-13) and one with grafted chains well below M_e (PS-105-6.7G-6). In Table 1 the graft PS are ordered according to these groups, with decreasing average number $\bar{p}$ of side chains per molecule.

The molar mass distribution of the side chains is narrow due to the anionic polymerization used to prepare the macromonomers; their molecular data shown in Table 1 were determined by SEC before copolymerization with styrene (Haug 2000). The number average mass fraction $\Phi_{n,br}$ of grafted side chains is obtained by

$$\Phi_{n,br} = \frac{\bar{p} \cdot M_{n,br}}{M_{n,bb} + \bar{p} \cdot M_{n,,br}} \quad (1)$$

where $\bar{p}$ denotes the average number of grafted branches per molecule and $M_{n,br}$ and $M_{n,bb}$ the number average molar masses of the grafted chains and the backbone, respectively. Values for $\Phi_{n,br}$ are summarized in Table 1. The mass-average molar masses for the graft polymers determined by static light scattering are also given in Table 1 together with the average molar masses and polydispersities from SEC.

To facilitate comparison with a linear polymer, a linear polystyrene (PS-r-95) with an average molar mass and molar mass distribution similar to the graft PS was prepared by free radical polymerization (molecular data in Table 1).

Typical SEC traces of the four branched samples with similar molar masses of the grafted side chains, but with different average numbers $\bar{p}$ of grafted side chains (PS-80-0.6G-22, PS-90-1.2G-27, PS-60-2.1G-27 and PS-70-3.2G-22) are shown in Fig. 2a. The graft PS with three different molar masses of the grafted side chains (PS-105-6.7G-6, PS-55-4.0G-13 and PS-60-1.4G-42) are shown in Fig. 2b together with the linear PS-r-95.

The low molar mass peaks are due to the residual linear macromonomers which did not react in the graft copolymer synthesis; the weight fractions $w_{MM} = m_{MM}/m_g$ of these low-molecular residues were substantially reduced by fractionated precipitation as proven by analysis of the SEC elution curves (Haug 2000). Values for w_{MM} are given in Table 1. Due to the similar molar masses of the macromonomers used for the graft PS as shown in Fig. 2a, their low-molecular weight residue peaks span a narrow window of molar masses. The molar masses of the macromonomers for the graft PS PS-105-6.7G-6, PS-55-4.0G-13 and PS-60-1.4G-42 are very different. The low-molecular residue peaks shown in Fig. 2b differ therefore clearly in molar mass.

To study the influence of the low-molecular weight residue content on rheological properties, the mass fraction of low-molecular weight residues was reduced after synthesis by precipitation for the samples PS-55-2.1G-27 and PS-90-1.2G-27, and was increased by an addition of low-molecular weight PS for the sample PS-60-0.5-55. As an example, the corresponding SEC-traces

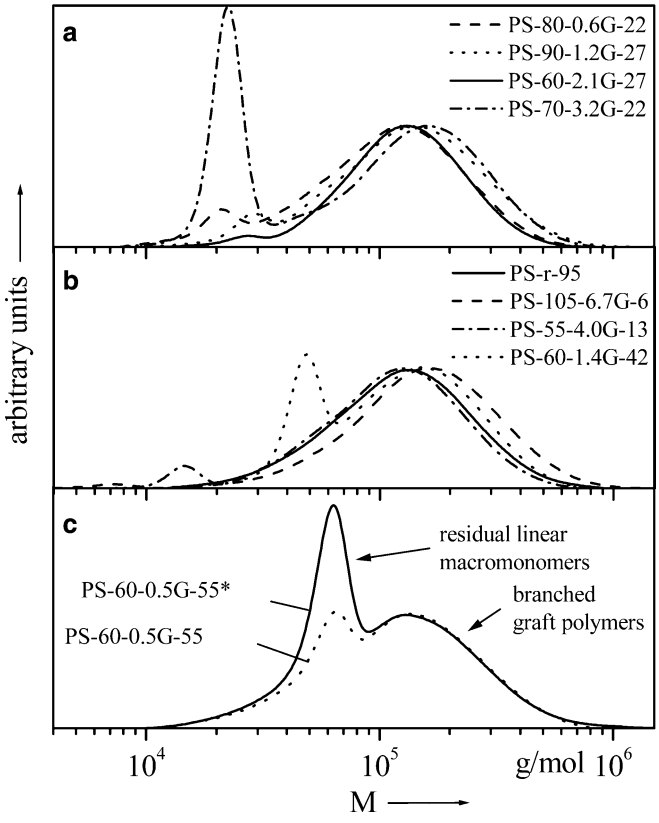

Fig. 2 Molecular weight distributions of graft PS. All distributions are normalized with respect to the peak maximum of the main peak. **a** Similar molecular weights of the grafted side chains, but different average number $\bar{p}$ of branches per molecule. **b** Different molecular weights of the grafted side chains. **c** Graft PS with different amounts of macromonomer residue. Mass fractions w_{MM} of the low-molecular weight residues are indicated in Table 1

are shown in Fig. 2c for PS-60-0.5G-55. The graft polymer constitution of PS-55-2.1G-27 was slightly changed by the precipitation, as indicated by the slightly higher backbone molar mass in Table 1. For the other two graft-polymers, the constitution was not changed due to precipitation; the samples with the higher amount of low-molecular weight residue are marked with a star.

Thermal stability of graft PS

During rheological measurements on melts, their viscosity might change due to thermal degradation. To get an insight into the thermal stability of the graft PS studied, the viscosities of the melts were measured over a time period exceeding the time needed to perform the frequency sweeps. Figure 3 shows the complex viscosities at the highest measuring temperature of 220°C for the melts of six graft PS with different average numbers and molar masses of grafted side chains. The values shown are related to the viscosity measured at the beginning of the test. A frequency in or near the terminal region of the melts was chosen to give a high sensitivity of the shear viscosity on molar mass changes. The viscosity decreases less than 5% within a measuring time of 30 min for PS-55-4.0G-13 and PS-70-3.2G-22. The viscosities of the other melts change less than 5% for a measuring time below 1 h.

The thermal stability was also checked by comparing the molar mass distributions of the powders as received and after the rheological experiments. As an example, three SEC-traces of PS-55-2.1G-27 are shown in the inset of Fig. 3: One SEC-trace of the powder, one after

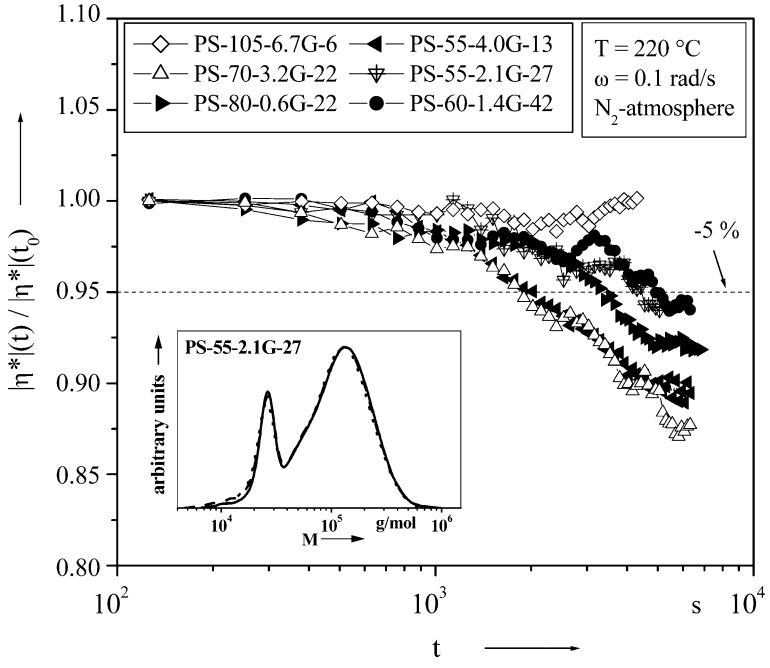

Fig. 3 Thermal stability at the highest measuring temperature of $T = 220$°C as tested by a time-sweep (dynamic measurement) for six branched PS with different molecular weights and average numbers of grafted side chains and by SEC for PS-55-2.1G-27 (*Solid line* powder, *broken line* after 2.5 h at 140–220°C, *dotted line* after 3 h at 220°C)

the rheological testing (2.5 h in a temperature range between 140°C and 220°C) and a third SEC-trace after the stability test at 220°C during 3 h. The molar mass average M_w of PS-55-2.1G-27 decreases by about 3% after the frequency sweeps and by about 4% after the stability test compared to the average molar mass of the powder, a change that is not significant within the experimental error of SEC measurements. The peak of the low-molecular weight residue does not increase after the rheological testing of the melts. This is an indication that side branches were not splitted by thermal activation during rheological testing. Therefore, it can be concluded that the results from rheological measurements reported here were not significantly affected by thermal degradation.

Frequency dependence of linear-viscoelastic functions

As the low-molar mass tail of the graft PS (cf. Fig. 2) which result from the residual linear PS might influence the frequency dependence of the dynamic moduli, a comparison of graft PS with different amounts of residues is shown in Fig. 4.

The graft polystyrenes PS-60-0.5G-55 with a low-molecular weight residue of $M_w = 5.83\times10^4$ g/mol and PS-90-1.2G-27 as well as PS-55-2.1G-27/PS-60-2.1G-27 with a low-molecular weight residue of $M_w = 2.87\times10^4$ g/mol were investigated. The dynamic moduli in Fig. 4 reveal that with a higher amount of low-molecular weight residue, the terminal zones of the dynamic moduli are shifted to higher frequencies for the three graft PS that were investigated. However, a two-step rubbery plateau is not observed for all the graft PS that were investigated. As shown on linear bimodal blends with narrow-distributed components, a two-step rubbery plateau with a second plateau (at low frequencies) can only be observed if the low-molar mass component is well entangled ($M_w >> M_c$), its weight fraction is sufficiently high, and the two components of the bimodal polymer are sufficiently separated (Watanabe et al. 1985; Montfort et al. 1986; Juliani and Archer 2001). The influence of the low-molecular weight residue on the frequency dependence of the dynamic moduli therefore results in a slight shift of the dynamic moduli to higher frequencies only.

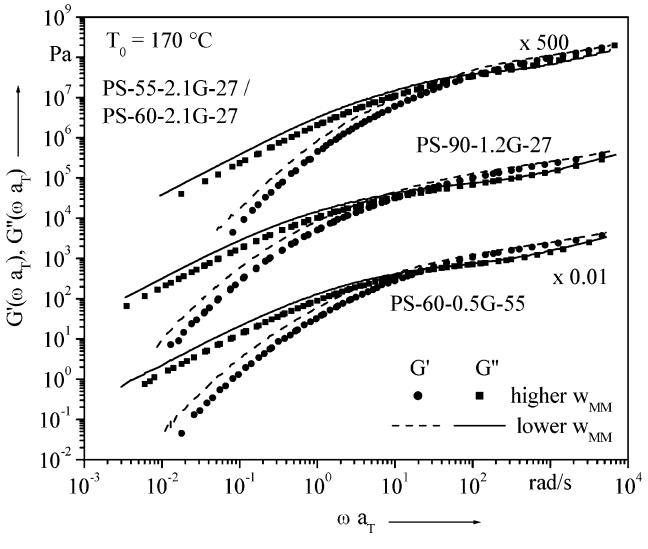

Fig. 4 Influence of the low-molecular weight macromonomer residue on the frequency dependence of the master curves of G' and G''. *Closed symbols*: higher amount w_{MM} of low-molecular weight residues, *lines*: lower amount w_{MM} of low-molecular weight residues. Mass fractions w_{MM} of the low-molecular weight residues are indicated in Table 1

The mastercurves of the storage and loss moduli of the graft PS with similar grafted side chain molar masses are shown in Fig. 5a, the ones with varying molar masses of grafted side chains in Fig. 5b. At low frequencies the terminal region with $G'\propto\omega^2$ and $G''\propto\omega$ is reached. In the high frequency region, the dynamic moduli become independent of the molar mass and the average number of branches. Due to the low molar mass of the graft PS, their entanglement density is small (on average approximately 7 to 13 entanglements per molecule) and the plateau region of the dynamic moduli is not well pronounced.

Most of the branched graft PS show a frequency dependence quite similar to that of the linear PS-r-95 which has a polydispersity comparable with that of the branched PS. This can readily be seen when comparing PS-r-95 and PS-90-1.2G-27 with similar zero-shear viscosities (Fig. 5a).

When the complex viscosities are plotted in the reduced form $|\eta*|/\eta_0 = f(\omega\cdot\eta_0)$, which according to Vinogradov (1980) is invariant of the molar mass and the reference temperature, the influence of the branching topology of the molecules on the frequency dependence of the dynamic viscosity ("shear thinning") can be compared, as the molar mass distributions of the main peaks of the graft PS (see Fig. 2, Table 1) are similar. The influence of the average number of grafted side chains is shown in Fig. 6a. Figure 6b shows graft PS with different molar masses and varying average numbers $\bar{p}$ of the grafted side chains, as well as a comparison of a graft polystyrene with different amounts w_{MM} of low-molecular weight residues. PS-60-0.5G-55 and PS-60-0.5G-55* with varying amounts of low-molecular weight residues possess a similar frequency dependence (Fig. 6b). The low-molecular weight residue of PS-60-0.5G-55 with the highest molar mass of $M_{w,MM} = 5.83\times10^4$ g/mol, which is well above $2M_e$, does not exhibit a significant influence on the reduced viscosity functions. This result can be interpreted in such a way that the low-molecular weight residues in our samples act as a low-molar mass additive, shifting the

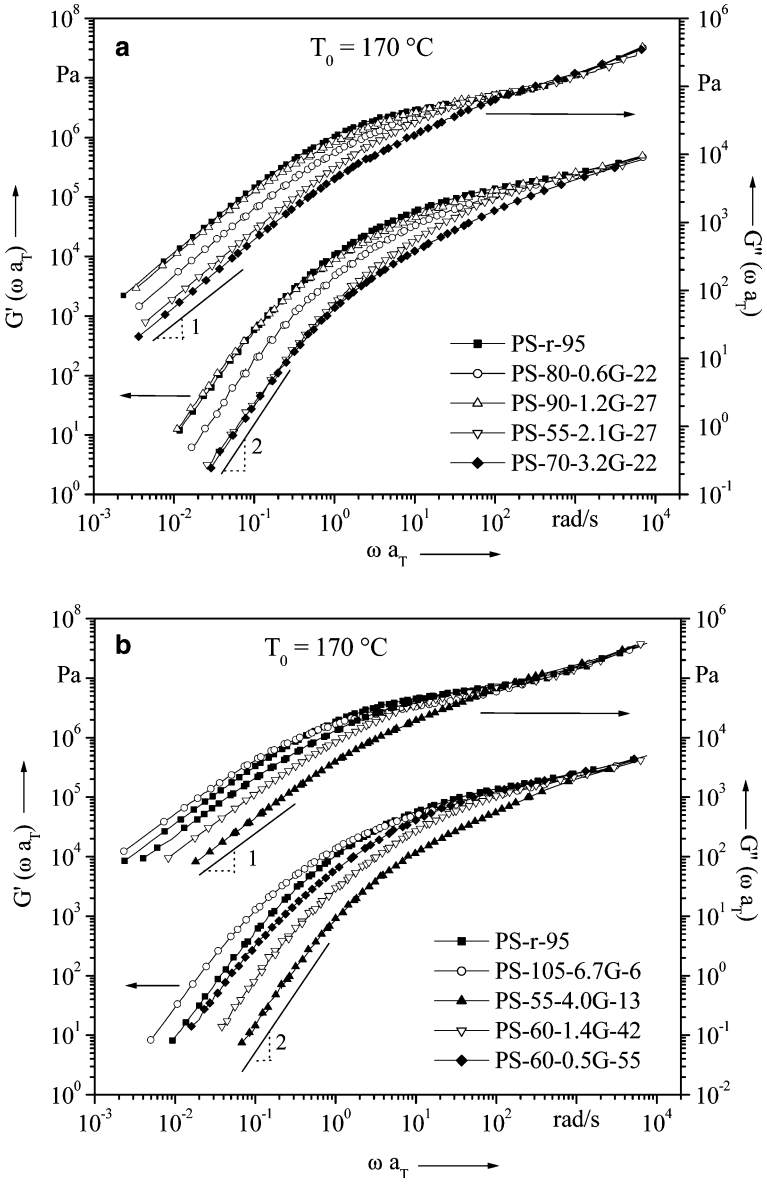

Fig. 5 Mastercurves of the dynamic moduli as a function of angular frequency for a linear polystyrene PS-r-95 and branched PS with **a** comparable molecular weights of the grafted side chains, but different average numbers of grafted side chains per molecule, **b** different molecular weights of grafted side chains. The reference temperature is $T_0 = 170°C$

dynamic moduli to lower frequencies but not significantly changing the frequency dependence of the reduced dynamic viscosity functions in the time window applied.

The reduced complex viscosity functions of the branched PS are very similar to the one of the linear PS-r-95, regardless of their average number of branches per molecule (Fig. 6a). PS-70-3.2G-22 and PS-60-2.1G-27 with a high average number of side chains per molecule show a slightly lower viscosity at intermediate frequencies and a slightly elevated viscosity at higher frequencies compared to the linear PS-r-95 (Fig. 6a). The same tendency can be seen for PS-55-4.0G-13, which exceeds the viscosity function of the linear PS at high frequencies (Fig. 6b). However, the graft polymers with longer grafted side chains (PS-60-1.4G-42 and PS-60-0.5G-55) as well as the one with very short branches (PS-105-6.7G-6) show a frequency dependence comparable to the one of the linear PS-r-95 (Fig. 6b).

Discussion of the frequency dependence of the dynamic moduli

In contrast to the current findings, data on a number of narrow-distributed branched model polymers show a very distinct relaxation mechanism between the terminal zone and the rubbery plateau, such as star-shaped polyisoprenes (Fetters et al. 1993), irregular star-shaped poly(ethylene-*alt*-propylene) (Gell et al. 1997),

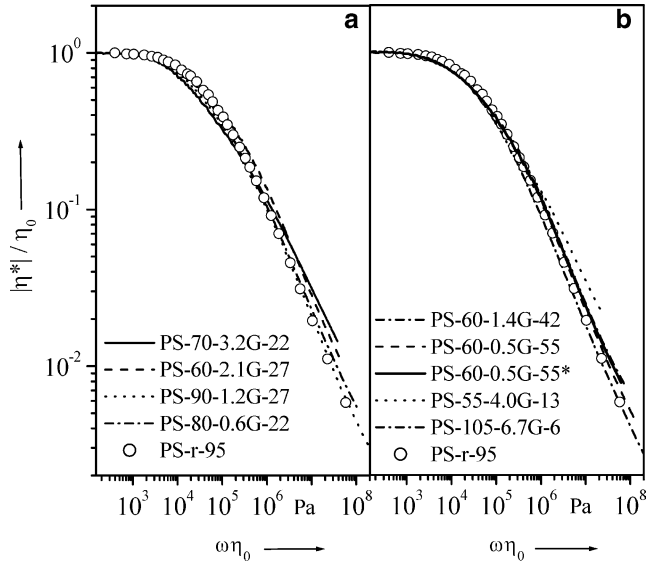

Fig. 6 Mastercurves of the reduced dynamic viscosities as a function of angular frequency ω multiplied by the zero-shear viscosity η_0 for the linear polystyrene PS-r-95 and branched PS with **a** comparable molecular weights of the grafted side chains, but a different average number of grafts per molecule, **b** different molecular weights of grafted side chains and different amounts of low-molecular weight residues. The reference temperature of the mastercurves is $T_0 = 170°C$

H-shaped PS (Roovers 1984), comb- and star-comb-shaped polybutadienes (Roovers and Toporowski 1987), and arborescent graft PS (Hempenius et al. 1998). This relaxation mechanism is generally seen by an increased value for G'' at frequencies higher than the crossover point ($G' = G''$) compared to the frequency dependence of the linear species. Even a Rouse-like behavior ($G' \propto \omega^{1/2}, G'' \propto \omega^{1/2}$) of the dynamic moduli in the transition between the terminal region and the plateau region has been found for narrow-distributed comb-PS by Roovers and Graessley (1981). These inflections are present even for combs with side branches of a molar mass well below $2M_e$ (Roovers and Graessley 1981). For comb- and star-PS, the width of this relaxation region depends on the arm molar mass (Graessley and Roovers 1979; Roovers and Graessley 1981). Similar results were shown for narrow-distributed asymmetrical stars, which have the same topology as a comb-polymer with a backbone and one single side chain at a position in the middle of the backbone. An asymmetrical star with a well-entangled backbone ($M_{bb}/M_e = 42$) but a slightly entangled side chain ($M_{br}/M_e = 2.4$) shows an inflection between the terminal zone and the rubbery plateau compared to the linear species (Gell et al. 1997). For regular, narrow-distributed star polymers, the reduced complex viscosity functions are the more frequency dependent the higher the molar masses of the stars are if compared to linear narrow-distributed PS (Graessley and Roovers 1979).

The topology of the graft PS with a low average number of the grafted side chains resembles that of a star, whereas for a higher average number $\bar{p}$ of grafts the topology is closer to a comb. For the graft PS studied in this work, the absence of a pronounced inflection of the dynamic moduli between the terminal zone and the rubbery plateau as well as the independence of the reduced complex viscosity functions on the number of side chains can therefore be interpreted such that the higher polydispersity of the graft PS in comparison to the samples in literature leads to a broader transition and may mask any effect of the grafted side chains on the frequency dependence (in contrast to literature data with narrow-distributed model polymers). These graft PS are therefore an example of branched topologies for which the effect of branches on the frequency dependence of linear-viscoelastic data is very weak.

Temperature dependence of linear-viscoelastic functions

By shifting the dynamic moduli, master curves are obtained, i.e., the time–temperature-superposition (TTS) is found to be valid for all graft PS that were investigated. For amorphous polymers not too far away from the glass transition, the WLF equation holds for the shift factors a_T (Ferry 1980):

$$\log\ a_T = -\frac{C_1(T - T_0)}{C_2 + (T - T_0)} \tag{2}$$

T_0 is the reference temperature and C_1 and C_2 are the WLF coefficients. The shift factors as a function of

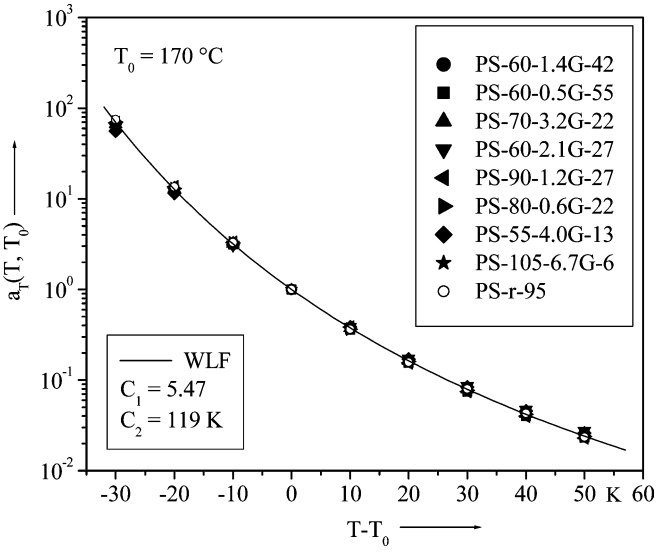

Fig. 7 Shift factors a_T from TTS of the data shown in Figs. 5 and 6. The line denotes the WLF equation with the value of its parameters as indicated. The reference temperature is $T_0 = 170°C$

temperature difference are shown in Fig. 7. Within experimental accuracy, the shift factors a_T are the same for all the graft PS that were investigated and correspond to that of the linear polystyrene PS-r-95.

The parameters C_1 and C_2 of the WLF equation derived from the data in Fig. 7 covering a temperature range from 140°C to 220°C are $C_1 = 5.47$ and $C_2 = 119$ K, at the reference temperature of $T_0 = 170$°C. These values are close to $C_1 = 5.49$ and $C_2 = 111.46$ K obtained by Lomellini (1992) for linear PS at a reference temperature of $T_0 = 170.6$°C or values from Ferry (1980) with $C_1 = 5.71$ and $C_2 = 120$ K, referred to a reference temperature of $T_0 = 170$°C. These findings mean that there is no dependence of the shift factors on the amount or length of the side branches for the graft polymers that were investigated.

Some other experimental studies on model PS with different topologies support these results: Fujimoto et al. (1970) found the shift factors to be independent of the density of branches and the branch molar mass for melts of comb-PS. Similar results were also obtained for comb-PS (Graessley and Roovers 1979), H-shaped PS (Roovers and Graessley 1981) and polystyrene stars (Masuda et al. 1971).

The lack of influence of branching on the temperature dependence of polystyrene melts is different from the findings on semi-crystalline polymers, for which a pronounced influence of branching on the temperature dependence was found, e.g., for polyethylenes (Laun 1987). This behavior becomes plausible from the following considerations: at temperatures near the glass transition, the free volume is decisive for molecular motions (Ferry 1980); at temperatures far away from the glass transition, the free volume is no longer considered as the rate-limiting factor and an Arrhenius-type temperature dependence is expected. For linear polystyrene, Lomellini (1992) found no evidence for an Arrhenius-like behavior up to a temperature of 290°C, indicating still an influence of the free volume on the temperature dependence of the shift factors up to $T \approx T_g + 190$°C. In a temperature range far above the glass transition, which is the case for polyethylenes in the molten state, the molecular mobility is no longer restricted by the availability of free volume. From the experimental findings it can be concluded that the influence of branches on the free volume is negligible in this temperature range that was tested.

Graessley (1982) points out that differences of the temperature coefficient due to long branches will only be obvious if the polymer does have a small temperature coefficient $-(d\ \ln a_T/\mathrm{d}T)$ and if the branches are well entangled, i.e. M_{br}/M_e is large. This result from literature supports our findings, as for the graft PS that were investigated, M_{br}/M_e is small ($M_{br}/M_e < 4$).

Viscoelastic quantities in the terminal zone

The zero-shear viscosities of all samples were determined according to $\eta_0 = \lim_{\omega \to 0}[G''(\omega)/\omega]$. Figure 8 shows the zero-shear viscosities as a function of mass-average molar mass which was determined by static light scattering for the branched samples. The values for η_0 at a reference temperature of $T_0 = 170$°C are collected in Table 2. The zero-shear-rate viscosities of the linear PS can be fitted by the function

$$\eta_0 = K \cdot M_w^{3.4} \tag{3}$$

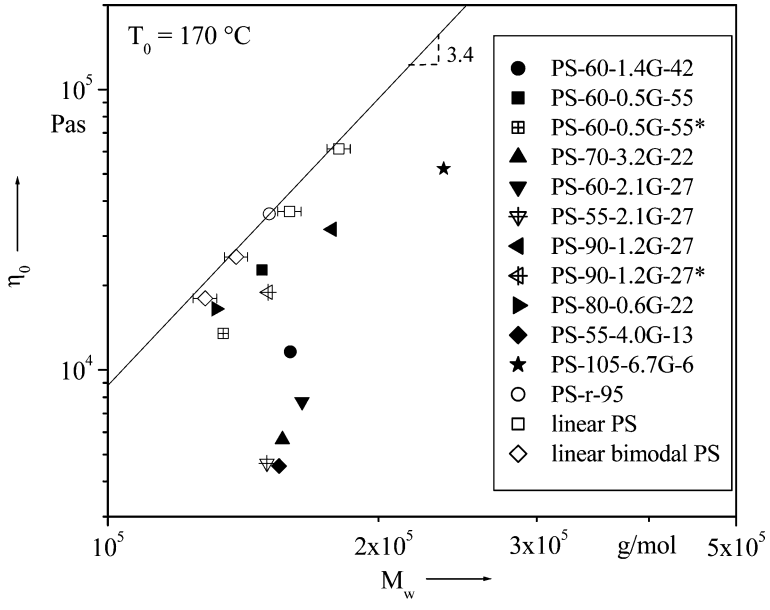

Fig. 8 Influence of branching on the zero-shear viscosity of the graft PS in comparison with linear PS. The mass-average molecular weight was determined from SEC data for the linear PS and via static light scattering for the graft PS. The *solid line* denotes the power law (Eq. 3) for linear PS. *Confidence bars* indicate a difference in M_w of ±3%. Linear bimodal PS denotes blends of PS-r-95 with 10 and 20 wt% of low-molecular weight PS ($M_w = 2.6 \times 10^4$ g/mol, $M_w/M_n = 1.05$)

Table 2 Zero-shear viscosities of the polystyrene melts at $T_0 = 170°C$ and contraction factor g' of dilute solutions (solvent: toluene, $T = 25°C$)

Sample	η_0 (Pa s)	$\eta_0/\eta_{0,\mathrm{lin}}^{a}$	$[\eta]^{b}$ (ml/g)	g'^{c}
PS-60-1.4G-42	11,600	0.27	48.8	0.78
PS-60-0.5G-55	22,700	0.67	52.8	0.89
PS-60-0.5G-55*	13,500	0.56	49.9	0.90
PS-70-3.2G-22	5,650	0.14	42.9	0.70
PS-60-2.1G-27	7,700	0.16	47.5	0.75
PS-55-2.1G-27	4,650	0.13	42.3	0.71
PS-90-1.2G-27	31,700	0.51	59.9	0.89
PS-90-1.2G-27*	18,900	0.53	53.0	0.88
PS-80-0.6G-22	16,500	0.73	51.1	0.94
PS-55-4.0G-13	4,550	0.12	42.9	0.72
PS-105-6.7G-6	52,200	0.32	64.0	0.78
PS-r-95	36,000	1	57.5	1

[a]Viscosity ratio calculated with the zero-shear viscosity of a linear polymer with identical molar mass
[b]Intrinsic viscosities in dilute solution (toluene). Data from Haug (2000)
[c]Ratio of intrinsic viscosities of the dilute solution $g' = [\eta]_{\mathrm{br}}/[\eta]_{\mathrm{lin}}$ with $[\eta]_{\mathrm{lin}}$ determined by Eq. 4. Data from Haug (2000)

with M_w in g/mol and $K = 8.8\times10^{-14}$ Pa s $(\mathrm{g/mol})^{-3.4}$ for a reference temperature of $T_0 = 170°C$ (Fig. 8). This relation is independent of the polydispersity as demonstrated by the fact that the η_0 values of the linear bimodal blends tend to lie on the curve for the other linear polystyrenes.

The influence of a low-molar mass residue on the zero-shear-melt viscosity was checked by a blend of PS-r-95 with 10 and 20 wt% of a low-molecular narrow-distributed PS which has a mass-average molar mass close to the one of the macromonomers ($M_w = 2.6\times10^4$ g/mol, $M_w/M_n = 1.05$). The linear PS-blends were prepared by Haug (2000) and are shown in Fig. 8, denoted as linear, bimodal PS. Their molar mass dependence of the zero-shear viscosities follows that one of the linear unimodal PS within experimental accuracy.

The zero-shear viscosities of all graft PS that were investigated are lower than those of the linear PS of the same molar mass (Fig. 8). The influence of branching structure on the viscosity decrease compared to linear molecules can be analyzed comparing the viscosity ratios $\eta_{0,\mathrm{br}}/\eta_{0,\mathrm{lin}}$ given in Table 2. The equivalent value $\eta_{0,\mathrm{lin}}$ for the linear PS was determined by Eq. 3 using the mass-average molar mass $M_{w,\mathrm{LS}}$ of the graft PS. The influence of branching on the viscosity decrease is shown in Fig. 9 by means of the viscosity ratio $\eta_{0,\mathrm{br}}/\eta_{0,\mathrm{lin}}$ as a function of the fraction of grafted side chains $\Phi_{n,\mathrm{br}}$ (for definition see Eq. 1). With the increasing fraction of grafted side chains $\Phi_{n,\mathrm{br}}$, the viscosity decrease of the branched chains compared to linear ones with the same molar mass is more pronounced. The parameter $\Phi_{n,\mathrm{br}}$ takes into account that even when side chains have similar molar masses, the average molecular weights of the backbones may be different, depending on the constitution of the graft polymer. The comparison of the pairs of graft PS with different weight fractions of macromonomers shows that for PS-60-2.1G-27/PS-55-2.1G-27 and PS-90-1.2G-27/PS-90-1.2G-27* the viscosity ratio $\eta_{0,\mathrm{br}}/\eta_{0,\mathrm{lin}}$ is about the same despite different weight fractions of the residual macromonomers. The graft polystyrene PS-60-0.5G-55* with a quite high macromonomer content of $w_{\mathrm{MM}} = 0.23$ shows a smaller viscosity ratio $\eta_{0,\mathrm{br}}/\eta_{0,\mathrm{lin}}$ than PS-60-0.5G-55 with $w_{\mathrm{MM}} = 0.07$. However, the differences are within the confidence bar for the viscosity ratio $\eta_{0,\mathrm{br}}/\eta_{0,\mathrm{lin}}$ as calculated from the change of $\eta_{0,\mathrm{lin}}$ by Eq. 3 with a difference of the mass-average molar mass of $\pm 3\%$.

With increased number or length of grafted side chains, the decrease in viscosity is more pronounced. The decrease of the zero-shear viscosity increases with a growing average number $\bar{p}$ of grafted side chains. This can be seen while comparing graft PS with similar molar masses of grafted side chains, but with a different average number of grafts per chain which are connected by the broken line in Fig. 9: The viscosity ratio $\eta_{0,\mathrm{br}}/\eta_{0,\mathrm{lin}}$ decreases from about 0.7 for PS-80-0.6G-22 for which every second molecule is branched on average to 0.5 for PS-90-1.2G-27 for which about every molecule is branched on an average to about 0.15 for the graft PS with about two and three grafts per chain (PS-60-2.1G-27 and PS-70-3.2G-22).

However, the viscosity decrease also depends on the length of the grafted side chains, as can be seen by the lower viscosity ratio of PS-70-3.2G-22 ($\eta_{0,\mathrm{br}}/\eta_{0,\mathrm{lin}} = 0.14$) with the shorter side chains compared to PS-60-1.4G-42

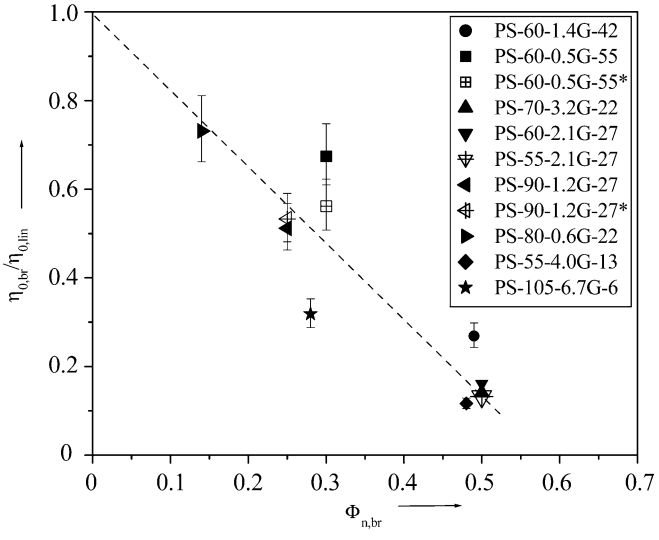

Fig. 9 Influence of branching on the viscosity ratio $\eta_{0,\mathrm{br}}/\eta_{0,\mathrm{lin}}$. *Confidence bars* indicate a difference in M_w of $\pm 3\%$. The *broken line* is drawn to guide the eye and connects samples with very similar molecular weights of the grafted side chains

with a similar fraction of grafted side chains $\Phi_{n,\mathrm{br}}$ but with longer side chains ($\eta_{0,\mathrm{br}}/\eta_{0,\mathrm{lin}} = 0.27$). The graft-polystyrene PS-105-6.7G-6 with shorter side chains of molar masses well below the entanglement molecular weight M_e shows also a lower viscosity ratio ($\eta_{0,\mathrm{br}}/\eta_{0,\mathrm{lin}} = 0.32$) compared to graft PS with a similar fraction of grafted side chains $\Phi_{n,\mathrm{br}}$, but with longer side chains, e.g., PS-60-0.5G-55* ($\eta_{0,\mathrm{br}}/\eta_{0,\mathrm{lin}} = 0.56$).

A decreased zero-shear viscosity in comparison to that of the linear PS with similar molar mass has also been found for randomly branched PS melts and solutions (Ferri and Lomellini 1999; Masuda et al. 1972). Fujimoto et al. (1970) found that the decrease in zero-shear viscosity for comb-branched polystyrene depends on the number of grafted side chains as well as on their molar mass. Qualitatively, similar results were found for comb-branched PS (Roovers and Graessley 1981; Fujimoto et al. 1972). With a fixed molar mass of the backbone and with increasing number of branches with the same molar mass, i.e., increasing $\Phi_{n,\mathrm{br}}$, the viscosity ratio $\eta_{0,\mathrm{br}}/\eta_{0,\mathrm{lin}}$ decreases for the combs studied by Roovers and Graessley (1981) and Fujimoto et al. (1972). The literature data therefore support our findings.

For 3-arm and 4-arm star polybutadiene melts, Kraus and Gruver (1965) showed that a reduced zero-shear viscosity for stars is only found at low molar masses. At high molar masses, the viscosities of the stars exceeded the ones of their linear counterparts with identical molar mass. Berry and Fox (1968) give an expression for the zero-shear viscosity, describing the viscosity enhancement as an exponential dependence of the zero-shear viscosity on the number of entanglements along the arms. This experimental evidence was also proved for polyisoprene stars by Graessley et al. (1976) and underlined by molecular theories (Pearson and Helfand 1984; Ball and McLeish 1989).

Two factors have to be considered when zero-shear viscosities of branched and linear chains are compared: One describes the reduction of the zero-shear viscosity due to the smaller radius of gyration of the branched polymers in comparison to the linear species of the same molar mass, the other deals with the viscosity enhancement found for example for star-polymers with very high molar masses. For 4-arm star PS, for example, Graessley and Roovers (1979) found that the melts of the star polymers do not exceed the zero-shear viscosities of linear PS up to a molar mass of about 10^6 g/mol, a molar mass at which the side chains of the stars are well entangled ($M_{w,\mathrm{br}}/M_e > 13$). With increasing functionality of star molecules, the molar mass at which the zero-shear viscosity of the stars exceeds one of the linear chains is even higher. The viscosity enhancement is attributed to a suppressed reptation, which is only present if the chains are sufficiently highly entangled (Roovers 1984). The fact that all graft PS that were investigated in this study show a decreased zero-shear viscosity in comparison to the linear molecules is an indication that the number of the entanglements of the side branches is not high enough to account for an increased viscosity compared to that of linear molecules with the same molar mass: the ratio $M_{w,\mathrm{br}}/M_e$ of all graft PS is less than four.

A measure for the reduced coil size in comparison to a linear chain is the factor $g' = [\eta]_{\mathrm{br}}/[\eta]_{\mathrm{lin}}$, i.e., the ratio of the intrinsic viscosity $[\eta]_{\mathrm{br}}$ of a graft polystyrene to the intrinsic viscosity of a linear PS. The intrinsic viscosities $[\eta]_{\mathrm{lin}}$ of linear PS are determined by

$$[\eta]_{\mathrm{lin}} = K_w M_w^a \tag{4}$$

[in units of ml/g with M_w in g/mol and with $K_w = 12.68\times10^{-3}$ ml/g (g/mol)$^{-a}$ and $a = 0.7096$ for toluene (Haug 2000)]. Values for g' are given in Table 2. An increasing number of grafted side chains with a similar side chain molar mass leads to a decreased ratio g', as can be seen while comparing PS-80-0.6G-22, PS-90-1.2G-27, PS-60-2.1G-27 and PS-70-3.2G-22. However, the reduction in coil size is not only influenced by the average number of grafts per chain but also by their length, as can be seen, e.g., while comparing PS-80-0.6G-22 ($g' = 0.94$) and PS-60-0.5G-55 ($g' = 0.89$) with a similar average number $\bar{p}$ of grafts, but with varying molar masses of grafted side chains.

Using the relations $\langle s^2 \rangle_0 \propto M$ and $[\eta]_\Theta \propto M^{1/2}$ of Fox and Flory (e.g. Flory 1988), the zero-shear viscosity can be expressed as a function of the unperturbed mean-square radius of gyration $\langle s^2 \rangle_0$, using Eq. 3:

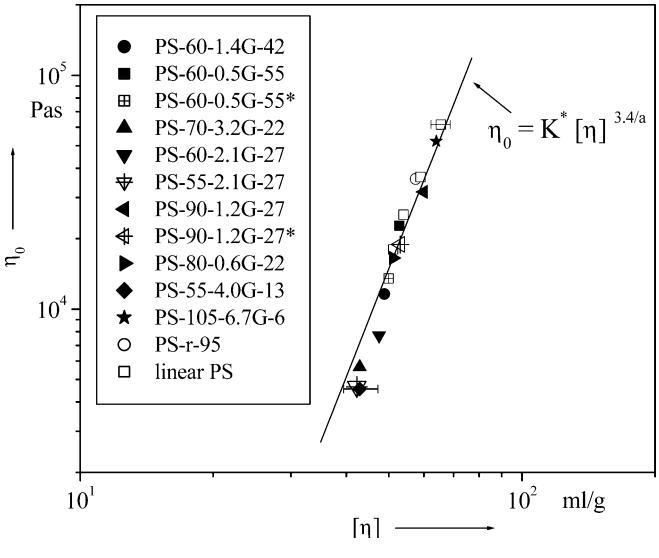

Fig. 10 Zero-shear viscosity ($T_0 = 170$°C) as a function of intrinsic viscosity of dilute solutions (solvent: toluene, $T = 25$°C). *Confidence bars* indicate an error of the intrinsic viscosity of ±5%. The *line* (according to Eq. 6) holds for linear PS with $a = 0.7096$ and $K^* = 1.08\times10^{-4}$ Pa s (ml/g)$^{(-3.4/a)}$

$$\eta_0 = K' \cdot \left(\langle s^2 \rangle_0\right)^{3.4} = K'' \cdot \left([\eta]_\Theta^2\right)^{3.4} \quad (6)$$

K' and K'' denote constant factors for a given polymer and solvent. For melts of branched molecules, the viscosity decrease due to the smaller radius of gyration caused by branching can be compensated by plotting the zero-shear viscosity η_0 as a function of the intrinsic viscosity $[\eta]_\Theta$ determined in Θ-solution, i.e., relating the zero-shear viscosity to the similar coil size of linear and branched chains (Roovers 1984; Roovers and Graessley 1981; Berry and Fox 1968). In this work, the intrinsic viscosities of the graft polymers were determined in the good solvent toluene (Haug 2000). The zero-shear viscosities of the graft polymers as a function of the intrinsic viscosities are shown in Fig. 10. Assuming that the coil dimensions of the branched chains increase in the same way as the ones of the linear chains when dissolved in a good solvent instead of a Θ-solvent, from Eqs. 3 and 4, the following correlation for linear PS is obtained:

$$\eta_0 = K \cdot M_w^{3.4} = K\left(\frac{[\eta]}{K_w}\right)^{\frac{3.4}{a}} = K^*[\eta]^{\frac{3.4}{a}} \quad (6)$$

With $a = 0.7096$ one gets the straight line with a slope of (3.4/0.7096) in the double logarithmic plot of Fig. 10. Within experimental accuracy, all graft PS follow the correlation for the linear PS. An increased zero-shear viscosity (“viscosity enhancement”), as observed for highly entangled combs, H-shaped and star-PS is not found (Graessley and Roovers 1979; Roovers 1984; Roovers and Graessley 1981). As an example, viscosity enhancement of the zero-shear viscosity as a function of intrinsic viscosity under Θ-conditions for regular stars is observed exceeding about four to five entanglements per arm for polystyrene 3-arm stars (Roovers 1984). The viscosity enhancement is attributed to a suppression of reptation when the side chains are very long.

The side chains of the graft PS studied in this work are only slightly entangled: the longest side chains of the graft polymers studied lead to only about three entanglements per chain (cf. Table 1). As a conclusion, the grafts of the branched PS studied here lead to a decrease in zero-shear viscosity which is caused by their smaller coil size; a viscosity enhancement due to long side chains is not observed.

Conclusions

Linear rheological properties of various model graft polystyrene melts with varying average numbers of grafted side chains per molecule ($0.5 \leq \bar{p} \leq 6.7$) and various molar masses of side chains are investigated using oscillatory shear measurements. A principal finding of the linear-viscoelastic properties of the graft PS is that the frequency dependence is primarily governed by the polydispersity of the graft PS ($M_w/M_n < 2.5$) rather than by the average number or the length of the slightly entangled grafted side chains ($M_{w,\mathrm{br}}/M_\mathrm{e} < 4$). This can readily be seen when plotting the dynamic viscosities in a normalized way independent of molar mass and temperature, which show that the frequency dependence of the complex viscosities of all graft PS is similar to the one of linear PS with a comparable polydispersity.

The smaller zero-shear viscosities of the graft PS compared to linear PS with the same molar mass can be related to the reduction of the coil diameter by branching. The reduction of the zero-shear viscosity depends more strongly on the number-average fraction $\Phi_{n,\mathrm{br}}$ of grafted side chains than on their total average number $\bar{p}$ alone.

The temperature dependence of $G'(\omega)$ and $G''(\omega)$ of the branched PS is the same as that of linear PS, which is in accordance with literature data of other branched PS.

In contrast to other studies on narrow-distributed model polymers like stars or combs, this work deals with model polymers where branching is associated with a polydisperse molar mass distribution, as is found for many commercially available polymers, like metallocene-catalyzed polyethylenes with a polydispersity of $M_w/M_n \cong 2$ (Gabriel and Münstedt 1999; Bin Wadud and Baird 2000). Due to the grafted side chains, the topology of the graft polymers that were investigated is closer to one of the statistical or tree-like branched structures that are present in highly branched commercial polymers (like LDPE) than to the simpler topologies of model polymers such as a star. Due to the stiffness of the polystyrene chain, the graft PS are not as much entangled as, e.g., polyethylene: A commercial polyethylene with $M_w = 1\times10^5$ g/mol has on average about 80 entanglements per chain, whereas the PS studied here have an entanglement density which is a factor of 10 lower.

The low-entanglement density of the graft PS explains the fact that the frequency-dependence of the reduced viscosity function is not altered by the grafted side chains and that the zero-shear viscosities are lower compared to a linear PS with similar molar mass.

Acknowledgements This work was supported by the German Research Foundation (DFG). Helpful discussions with Dr. J. Kaschta, Dr. C. Gabriel and Dr. K. Dirnberger are gratefully acknowledged. P.K.H. would like to thank the Fonds der Chemischen Industrie for granting a fellowship.

References

Ball RC, McLeish TCB (1989) Dynamic dilution and the viscosity of star polymer melts. Macromolecules 22:1911–1913

Beigzadeh D, Soares JBP, Hamielec AE (1999) Recipes for synthesizing polyolefins with tailor-made molecular weight, polydispersity index, long-chain branching frequencies, and chemical composition using combined metallocene catalyst systems in a CSTR at steady state. J Appl Polym Sci 71:1753–1770

Berry GC, Fox TG (1968) The viscosity of polymers and their concentrated solutions. Adv Polym Sci 5:261–357

Bin Wadud SE, Baird DG (2000) Shear and extensional rheology of sparsely branched metallocene-catalyzed polyethylenes. J Rheol 44:1151–1167

Daniels DR, McLeish TCB, Crosby BJ, Young RN, Fernyhough CM (2001) Molecular rheology of comb polymer melts. 1. Linear viscoelastic response. Macromolecules 34(20):7025–7033

Ferri D, Lomellini P (1999) Melt rheology of randomly branched polystyrenes. J Rheol 43:1355–1372

Ferry JD (1980) Viscoelastic properties of polymers. Wiley, New York

Fetters LJ, Kiss AD, Pearson DS, Quack GF, Vitus FJ (1993) Rheological behavior of star-shaped polymers. Macromolecules 26:647–654

Flory PJ (1988) Statistical mechanics of chain molecules. Hanser, Munich, Vienna, New York

Fujimoto T, Kajiura H, Hirose M, Nagasawa M (1970) Viscoelastic properties of comb-shaped polystyrenes. Macromolecules 3:57–64

Fujimoto T, Kajiura H, Hirose M, Nagasawa M (1972) Viscoelastic properties of comb-shaped polystyrenes having parent polymers of different molecular weights. Polym J 3:181–188

Gabriel C, Münstedt H (1999) Creep recovery behavior of metallocene linear low-density polyethylenes. Rheol Acta 38:393–403

Gell CB, Graessley WW, Efstratiadis V, Pitsikalis M, Hadjichristidis N (1997) Viscoelasticity and self-diffusion in melts of entangled asymmetric star polymers. J Polym Sci Polym Phys 35:1943–1954

Graessley WW (1982) Effect of long branches on the temperature dependence of viscoelastic properties in polymer melts. Macromolecules 15:1164–1167

Graessley WW, Roovers J (1979) Melt rheology of four-arm and six-arm star polystyrenes. Macromolecules 12:959–965

Graessley WW, Masuda T, Roovers J, Hadjichristidis N (1976) Rheological properties of linear and branched polyisoprene. Macromolecules 9:127–141

Harrison D, Coulter IM, Wang SH, Nistala S, Bradley AK, Pigeon M, Tian J, Collins S (1998) Olefin polymerization using supported metallocene catalysts: development of high activity catalysts for use in slurry and gas phase ethylene polymerizations. J Mol Catal A Chem 128:65–77

Haug PK (2000) Polystyrol-Pfropfpolymere definierter Struktur als Modellsystem für Langkettenverzweigungen in Polyolefinen. PhD Thesis, University Stuttgart

Hempenius MA, Zoetelief WF, Gauthier M, Möller M (1998) Melt rheology of arborescent graft polystyrenes. Macromolecules 31:2299–2304

Hepperle J (2002) Einfluss der molekularen Struktur auf rheologische Eigenschaften von Polystyrol- und Polycarbonatschmelzen. PhD Thesis, University Erlangen-Nürnberg

Islam MT, Juliani J, Varshney SK, Archer LA (2001) Linear rheology of entangled six-arm and eight-arm polybutadienes. Macromolecules 34:6438–6449

Juliani J, Archer LA (2001) Linear and nonlinear rheology of bidisperse polymer blends. J Rheol 45:691–708

Kraus G, Gruver JT (1965) Rheological properties of multichain polybutadienes. J Polym Sci A 3:105–122

Kurzbeck S, Oster F, Münstedt H, Nguyen TQ, Gensler R (1999) Rheological properties of two polypropylenes with different molecular structure. J Rheol 43:359–374

Laun HM (1987) Orientation of macromolecules and elastic deformations in polymer melts. Influence of molecular structure on the reptation of molecules. Prog Colloid Polym Sci 75:111–139

Lee JH, Archer LA (2002) Stress relaxation of star/linear polymer blends. Macromolecules 35:6687–6696

Lomellini P (1992) Williams-Landel-Ferry versus Arrhenius behaviour: polystyrene melt viscoelasticity revised. Polymer 33:4983–4990

Masuda T, Ohta Y, Onogi S (1971) Rheological properties of anionic polystyrenes. III. Characterization and rheological properties of four-branch polystyrenes. Macromolecules 4:763–768

Masuda T, Nakagawa Y, Ohta Y, Onogi S (1972) Viscoelastic properties of concentrated solutions of randomly branched polystyrenes. Polym J 3:92–99

Montfort JP, Marin G, Monge Ph (1986) Effect of tube renewal on the viscoelastic properties of concentrated solutions of polymers. Macromolecules 19:393–399

Münstedt H, Laun HM (1981) Elongational properties and molecular structure of polyethylene melts. Rheol Acta 20:211–221

Odian G (1991) Principles of polymerization, 3rd edn. Wiley, New York

Pearson DS, Helfand E (1984) Viscoelastic properties of star-shaped polymers. Macromolecules 17:888–895

Pearson DS, Mueller SJ, Fetters LJ, Hadjichristidis N (1983) Comparison of the rheological properties of linear and star-branched polyisoprenes in shear and elongational flows. J Polym Sci Polym Phys Ed 21:2287–2298

Pryke A, Blackwell RJ, McLeish TCB, Young RN (2002) Synthesis, hydrogenation, and rheology of 1,2-polybutadiene star polymers. Macromolecules 35:467–472

Roovers J (1984) Melt rheology of H-shaped polystyrenes. Macromolecules 17:1196–1200

Roovers J, Graessley WW (1981) Melt rheology of some model comb polystyrenes. Macromolecules 14:766–773

Roovers J, Toporowski PM (1987) Relaxation by constraint release in combs and star-combs. Macromolecules 20:2300–2306

Tobita H (1999) Comb-branched polymer formation during copolymerization with macromonomer. Polym React Eng 7:577–605

Vinogradov GV (1980) Rheology of polymers. Mir Publishers, Moskau

Watanabe H, Sakamoto T, Kotaka T (1985) Viscoelastic properties of binary blends of narrow molecular weight distribution polystyrenes 2. Macromolecules 18:1008–1015